

REPORT



YTH domain family 2 orchestrates epithelial-mesenchymal transition/proliferation dichotomy in pancreatic cancer cells

Jixiang Chen^{a,†}, Yaocheng Sun^{a,†}, Xiao Xu^b, Dawei Wang^c, Junbo He^c, Hailang Zhou^c, Ying Lu^c, Jian Zeng^b, Fengyi Du^b, Aihua Gong^b, and Min Xu^c

^aDepartment of General Surgery, Affiliated Hospital of Jiangsu University, Jiangsu University, Zhenjiang, Jiangsu, China; ^bDepartment of Cell Biology, School of Medicine, Jiangsu University, Zhenjiang, Jiangsu, China; ^cDepartment of Gastroenterology, Affiliated Hospital of Jiangsu University, Jiangsu University, Zhenjiang, Jiangsu, China

ABSTRACT

Recent studies show that YTH domain family 2 (YTHDF2) preferentially binds to m⁶A-containing mRNA regulates localization and stability of the bound mRNA. However, the role of YTHDF2 in pancreatic cancers remains to be elucidated. Here, we find that YTHDF2 expression is up-regulated in pancreatic cancer tissues compared with normal tissues at both mRNA and protein levels, and is higher in clinical patients with later stages of pancreatic cancer, indicating that YTHDF2 possesses potential clinical significance for diagnosis and prognosis of pancreatic cancers. Furthermore, we find that YTHDF2 orchestrates two cellular processes: promotes proliferation and inhibits migration and invasion in pancreatic cancer cells, a phenomenon called “migration-proliferation dichotomy”, as well as epithelial-mesenchymal transition (EMT) in pancreatic cancer cells. Furthermore, YTHDF2 knockdown significantly increases the total YAP expression, but inhibits TGF- β /Smad signaling, indicating that YTHDF2 regulates EMT probably via YAP signaling. In summary, all these findings suggest that YTHDF2 may be a new predictive biomarker of development of pancreatic cancer, but a serious consideration is needed to treat YTHDF2 as a target for pancreatic cancer.

ARTICLE HISTORY

Received 9 January 2017
Revised 8 September 2017
Accepted 11 September 2017

KEYWORDS

EMT; migration-proliferation dichotomy; pancreatic cancer; YAP; YTHDF2

Introduction


Pancreatic cancer is one of the most aggressive and lethal malignancies.¹ It is projected to become the second most common cause of cancer deaths in the United States by 2020.² Despite decades of effort, the five-year survival rate remains at only ~5%.³ Pancreatic cancer is usually diagnosed at an advanced stage due to a lack of symptoms in the early stages so that resection of the advanced tumor is often not possible.⁴ Thus, it is of great significance to look for new therapeutic targets for this disease.

N⁶-methyl-adenosine modification in mRNA (m⁶A) is extremely widespread which functionally modulates the eukaryotic transcriptome to influence mRNA splicing, export, localization, translation and stability.⁵ Cellular components of m⁶A methylation have long been known to be intimately linked to cancer. For instance, high incidence of prostate cancer, breast cancer and pancreatic cancer could also be linked to allelic variants of FTO (m⁶A demethylase). Phosphorylation of METTL3 (m⁶A methylase) could be correlated to tumorigenesis.⁶ Recently, a m⁶A-specific reader, YTH domain family, including YTHDF1-3, YTHDC1, YTHDC2, YTHDF2 specifically binds to m⁶A-containing mRNA via its C-terminal YTH domain and thereby confers various downstream fates of bound RNAs.^{7–9} Depletion of

YTHDF2 protein gives rise to an increase in both abundance and half lives of cellular mRNAs, indicating the stability of mRNAs is inversely correlated to the number of YTHDF2 binding sites present in target mRNAs.⁶ One study shows that YTHDF2 is a translocation partner of RUNX1 in acute myeloid leukemia patients.¹⁰ Taken together, it is well-established that cellular components of m⁶A methylation are involved in cancer carcinogenesis and may serve as tumor promoters or suppressors. However, the specific roles and underlying mechanisms of YTHDF2 in cancers are still unknown.

The present study was aimed to determine the expression of YTHDF2 in pancreatic cancer, and to investigate the effects of YTHDF2 on proliferation, migration and invasion in pancreatic cancer cells. Our data show that YTHDF2 is up-regulated in human pancreatic cancer at both mRNA and protein levels and orchestrates proliferation and epithelial-mesenchymal transition dichotomy in pancreatic cancer cells. Furthermore, YTHDF2 knockdown promotes EMT probably via up-regulation of YAP but not TGF- β /Smad signaling in pancreatic cancer cells. Our study for the first time found that YTHDF2 might play an important role in pancreatic cancer progression, and interestingly might display dual effects in the disease.

CONTACT Professor Aihua Gong ✉ ahg5@mail.uj.edu.cn 301 Xuefu Road, Zhenjiang, 212013, Jiangsu, China; Professor Min Xu ✉ peterxu1974@163.com
438 Jiefang Road, Zhenjiang, 212013, Jiangsu, China.

 Supplemental data for this article can be accessed on the [publisher's website](#).

[†] These authors contributed equally to this work.

Results

YTHDF2 is up-regulated in pancreatic cancer and associated with patients' poor stage

To confirm the clinical relevance of YTHDF2 expression, we first analyzed the YTHDF2 protein expression in clinical specimens from the human protein atlas (www.proteinatlas.org). We observed strong YTHDF2 staining in pancreatic cancer, but very weak staining in normal pancreas (Fig. 1A). Consistently, YTHDF2 mRNA level was lower in normal pancreatic tissues than that in pancreatic cancer tissues (9.014 ± 0.09101 vs. 9.274 ± 0.05050 , $P < 0.001$, $n = 52$) in the Gene Expression Omnibus (GEO) (Fig. 1B). As there is no relevant clinical data in GEO, we further interrogated TCGA data base to evaluate the correlation of YTHDF2 expression with patients' clinical stages (<https://genome-cancer.ucsc.edu>). The analysis showed that YTHDF2 expression increased successively in stage I, stage II, stage III and stage IV groups, and the stage I group presented the lowest and stage IV the highest YTHDF2 expression levels (Fig. 1C). Moreover, YTHDF2 expression in Pathologic T1 and T2 was lower than that in Pathologic T3 and T4 (Fig. 1D). All these data suggest that YTHDF2 is up-regulated in pancreatic cancer and associated with the poor stage of patients.

YTHDF2 expression is profiled in pancreatic cancer cells

To conduct the next experiments in pancreatic cancer cells, we first examined the expression level of YTHDF2 in PaTu8988, SW1990 and BxPC3 cells using real-time PCR and western blot. We noticed that YTHDF2 expression, at both mRNA and protein levels, was higher in SW1990 and BxPC3 cells (Fig. 2A). Subsequently, we constructed sh-YTHDF2 plasmids to investigate the roles of YTHDF2 in pancreatic cancer, sh-EGFP as a control. After transfection, the mRNA and protein levels of YTHDF2 significantly reduced in sh-YTHDF2 group compared with sh-EGFP group (Fig. 2B). Vector or Flag-YTHDF2 was transferred into SW1990 and PaTu8988 cells, and then YTHDF2 overexpression was examined at mRNA by real-time PCR (Fig. S1A). Unexpectedly, no significant changes in the level of protein were observed in YTHDF2 overexpression group (Fig. S1B). Subsequently, we identified plasmids Vector and Flag-YTHDF2 in H293T cell, the mRNA and protein levels of YTHDF2 were significantly increased in Flag-YTHDF2 group compared with Vector group (Fig. S1C). The reason that YTHDF2 overexpression could not be at the protein levels in pancreatic cancer cells is not clear and no significant changes in cellular function were observed (data not shown). Therefore, we had not made an attempt at the overexpression in the subsequent experiments.

YTHDF2 knockdown inhibits the ability of proliferation via Akt/GSK3 β /CyclinD1 pathway in pancreatic cancer cells

To determine whether YTHDF2 expression was required for the proliferation in pancreatic cancer cells, SW1990 and BxPC3 cells were transfected with sh-EGFP or sh-YTHDF2 and proliferation ability was evaluated using colony formation assay. We found that YTHDF2 knockdown resulted in the smaller

colonies and lower colony density compared to the control group in both SW1990 and BxPC3 cells (438 ± 18 vs. $155 \pm 12/ 201 \pm 15$ and 514 ± 12 vs. $206 \pm 11/ 248 \pm 16$, $P < 0.001$, Fig. 3A), indicating that the ability of cell colony formation was significantly suppressed by YTHDF2 depletion. Subsequently, we used the CCK8 assay to detect the growth curves. YTHDF2 knockdown resulted in the inhibition of proliferation in SW1990 and BxPC3 cells at 2, 3, 4, 5 and 6 days after transfection (Fig. 3B). Also, YTHDF2 knockdown led to down-regulation of p-GSK3 β and CyclinD1 at protein levels in SW1990 and BxPC3 cells (Fig. 3C). Many other protein kinases are capable of phosphorylating GSK-3 β , such as Akt, ILK and PKA.¹¹ Our data suggested that YTHDF2 knockdown resulted in down-regulation of p-Akt and had no influence on total Akt, total GSK3 β , ILK, total PKA, p-PKA protein (Fig. 3C, Fig. S1D). YTHDF2 knockdown increased the fraction of cells in G1/G0-phase with a corresponding decrease in S-phase as compared to the control in SW1990 and BxPC3 cells, indicating a potential role of YTHDF2 knockdown in G1 arrest (Fig. 3D, E). These results reveal that YTHDF2 knockdown inhibits the ability of proliferation possibly via Akt/GSK3 β /CyclinD1 pathway in pancreatic cancer cells.

YTHDF2 knockdown promotes the migration ability of pancreatic cancer cells

Next, we then explored the effects of YTHDF2 on the migration of pancreatic cancer cells. To test the effects of YTHDF2 knockdown on cell motility, we examined the migratory potential of SW1990 and BxPC3 cells by using a transwell assay. We found that the numbers of migrated cells were 173 ± 15 and 417 ± 25 in sh-EGFP and sh-YTHDF2#1 SW1990 cells, and 112 ± 8 and 298 ± 18 in sh-EGFP and sh-YTHDF2#1 BxPC3 cells, respectively (Fig. 4A, B), indicating that YTHDF2 knockdown improved the ability of migration in SW1990 and BxPC3 cells. To confirm the above results, we also performed wound-healing assays (scratch assays, Fig. 4C, D). For these assays, a scrape wound was created on confluent cultures of SW1990 and BxPC3 cells expressing either sh-EGFP or sh-YTHDF2#1. SW1990 or BxPC3 cells expressing sh-YTHDF2#1 displayed increased motility in comparison to SW1990 or BxPC3 cells expressing sh-EGFP ($11.5 \pm 0.7\%$ vs. $31.5 \pm 2.1\%$ and $13 \pm 1.4\%$ vs. $30 \pm 2.8\%$, $P < 0.001$, Fig. 4C, D). All these results suggest that YTHDF2 knockdown promotes the ability of migration in pancreatic cancer cells.

YTHDF2 knockdown promotes the invasion and adhesion ability in pancreatic cancer cells

Subsequently, we examined the ability of invasion by BD Matrigel invasion assays. SW1990 and BxPC3 cells were transfected with sh-EGFP or sh-YTHDF2#1 plasmids. The numbers of invasive cells were 68 ± 8 and 188 ± 8 in sh-EGFP and sh-YTHDF2#1 SW1990 cells, and 78 ± 8 and 226 ± 13 in sh-EGFP and sh-YTHDF2#1 BxPC3 cells, respectively (Fig. 5A, B), indicating that knockdown of YTHDF2 obviously enhanced the invasion ability of SW1990 and BxPC3 cells. Also, YTHDF2 knockdown led to up-regulation of MMP2 and MMP9 at both mRNA and protein levels in

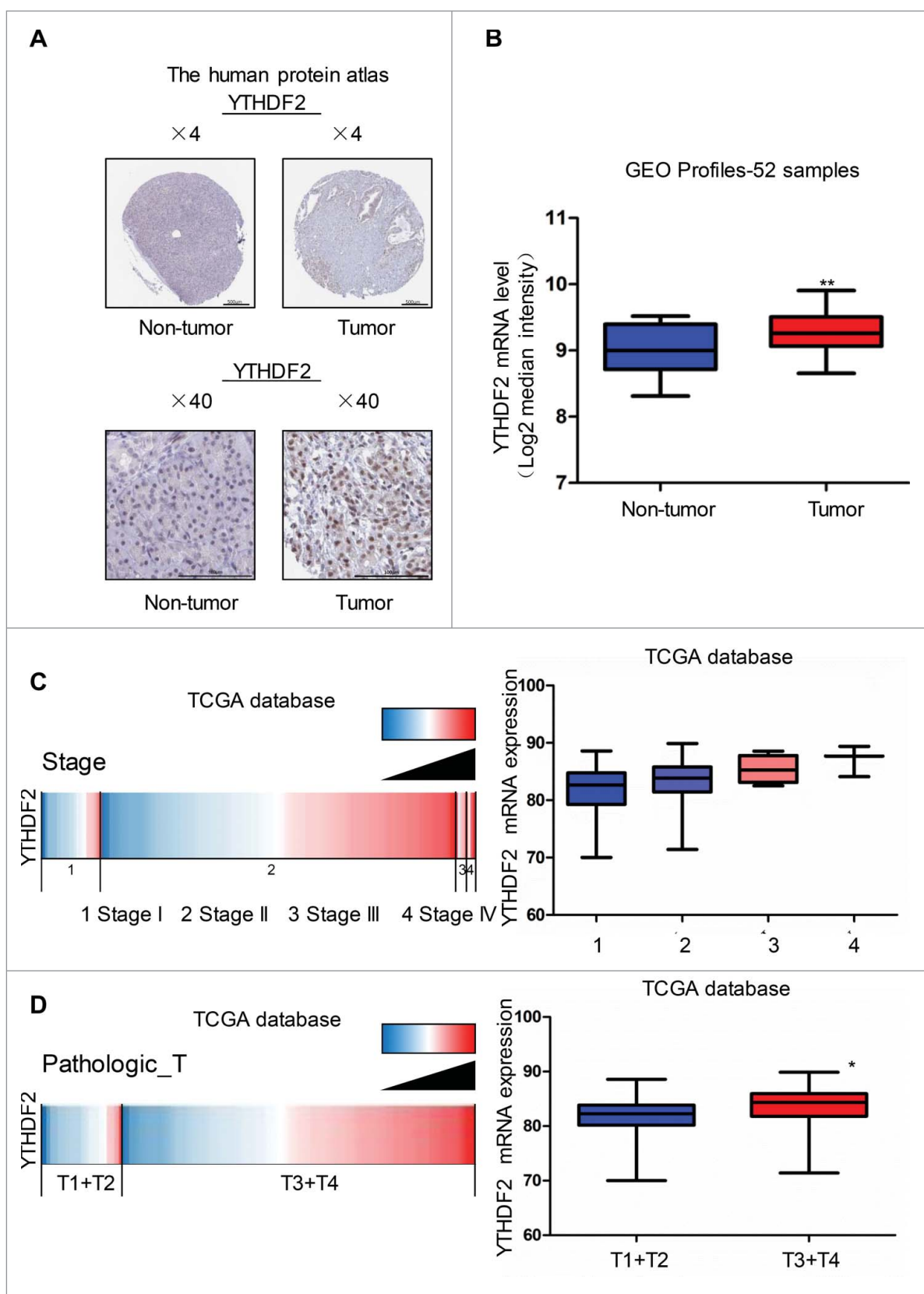


Figure 1. YTHDF2 is up-regulated in pancreatic cancer and associated with patients' poor stage. (A) YTHDF2 protein expression in pancreatic cancer tissues and normal pancreatic tissues was analyzed through the human protein atlas (www.proteinatlas.org). Magnification, $\times 4$; bars, $500 \mu\text{m}$. Magnification, $\times 40$; bars, $100 \mu\text{m}$. (B) Analysis of YTHDF2 mRNA levels in 52 samples of pancreatic cancer and non-tumor tissues in the Gene Expression Omnibus. $N = 16$ for non-tumor group, and $N = 36$ for tumor group. $**P < 0.01$. (C) Analysis of the TCGA database indicates YTHDF2 is associated with stage in pancreatic cancer. $N = 20$ for stage I group, $N = 140$ for stage II group, and $N = 4$ for stage III group, and $N = 3$ for stage IV group. $*P < 0.05$. (D) Analysis of the TCGA database indicates YTHDF2 is associated with PathologicT in pancreatic cancer. $N = 27$ for PathologicT1 and T2, $N = 140$ for PathologicT3 and T4. $*P < 0.05$.

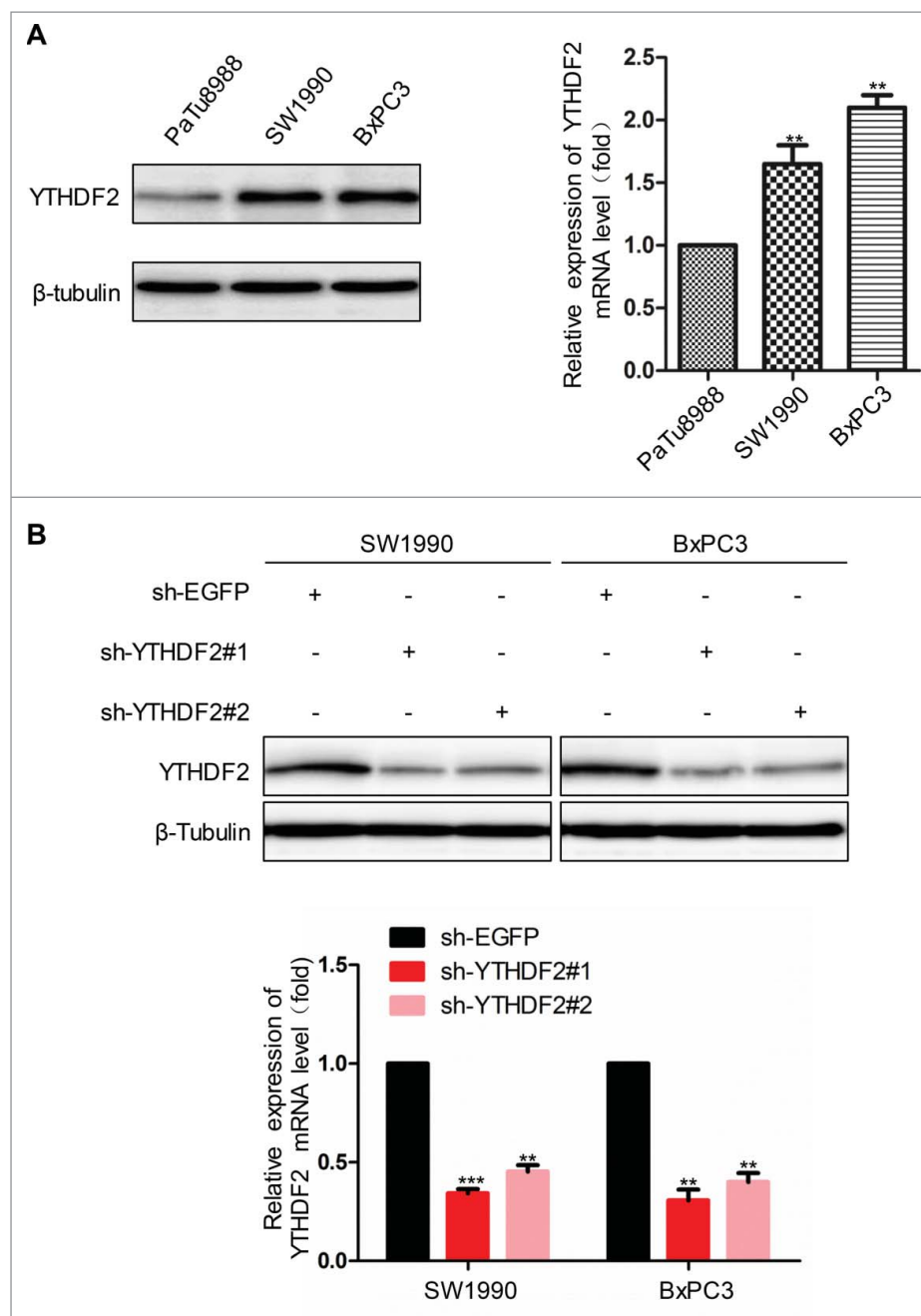


Figure 2. YTHDF2 Expression in different pancreatic cancer cells. (A) Relative expression levels of YTHDF2 protein and mRNA were assessed in PaTu8988, SW1990 and BxPC3 cells. (B) YTHDF2 protein and mRNA levels were decreased after sh-YTHDF2#1 and sh-YTHDF2#2 was transfected into SW1990 and BxPC3 cells. *** $P < 0.001$. Data are expressed as mean \pm SD. The results are representative of three independent experiments.

SW1990 and BxPC3 cells (Fig. 5C, D). Furthermore, we found that YTHDF2 knockdown resulted in the stronger adhesion ability compared to the control group in both SW1990 and BxPC3 cells ($P < 0.05$ and $P < 0.01$, Fig. 5E). Above all data suggest that YTHDF2 knockdown promotes the invasion and adhesion ability in pancreatic cancer cells.

YTHDF2 knockdown promotes EMT via YAP signaling

Previous study has shown that the EMT is associated with the abilities of migration and invasion in cancer cells.¹² Therefore, we detected the EMT markers at protein levels using western blotting. Our results revealed that YTHDF2 knockdown

induced down-regulation of E-cadherin and up-regulation of Vimentin, Snail (Fig. 6A). Actually, TGF- β induces EMT in many cancers.^{13,14} Thus, we investigated the effects of YTHDF2 on the classic TGF- β /Smad signaling. Surprisingly, we found that YTHDF2 knockdown down-regulated mature TGF- β , Smad2/3, p-Smad2 in SW1990 and BxPC3 cells and thereby inhibited TGF- β /Smad signaling (Fig. 6B), indicating that YTHDF2 knockdown-induced EMT was driven by other pathways. Recently, it is reported that YAP is closely related to EMT in cancer.¹⁵ Next, we investigated the effects of YTHDF2 on the classic Hippo signaling in pancreatic cancer cells. The results showed that YTHDF2 knockdown down-regulated the LATS1, p-LATS1, MOB1, p-MOB1 and up-regulated the total

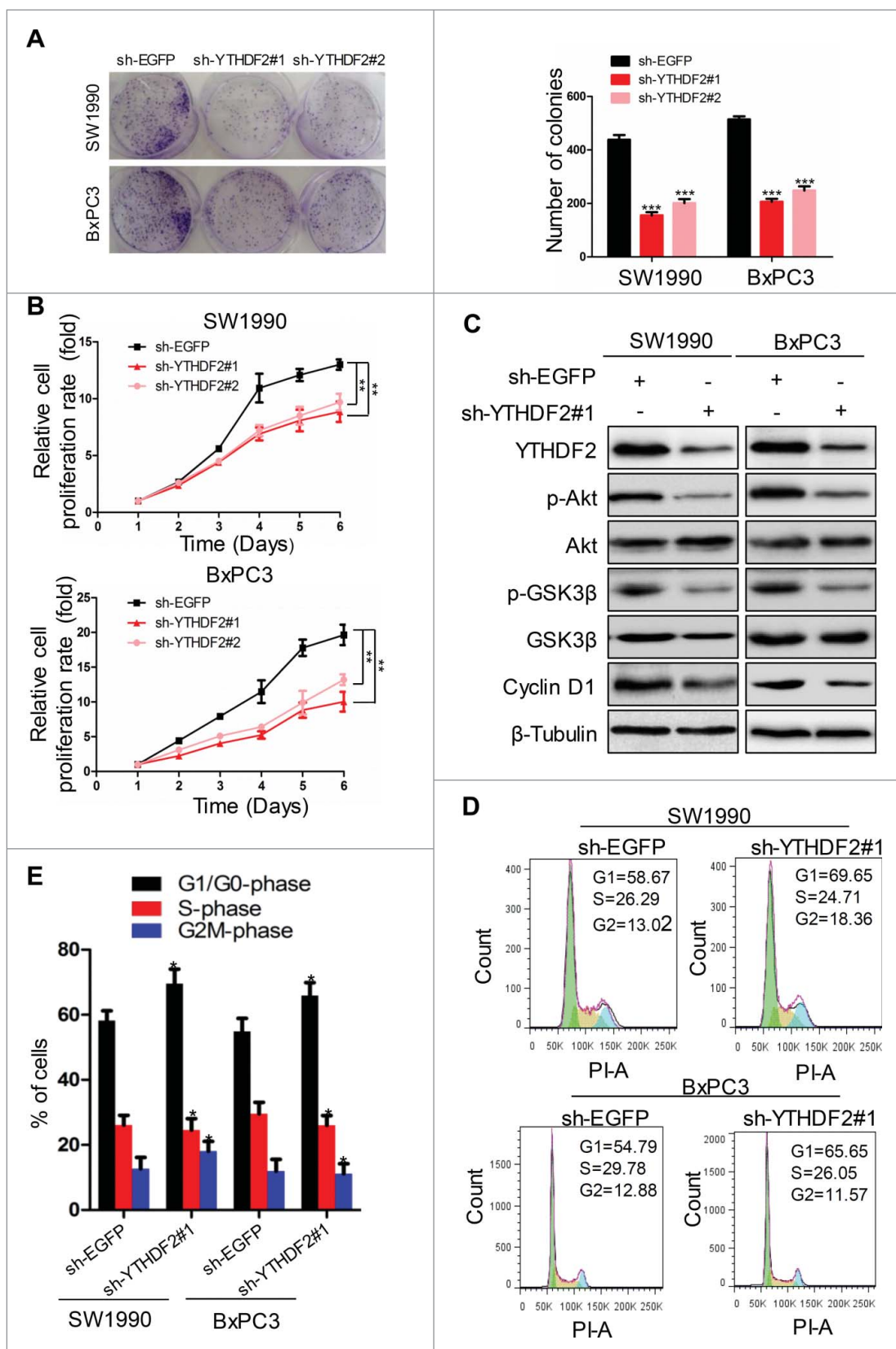


Figure 3. YTHDF2 knockdown inhibits the ability of proliferation via Akt/GSK3 β /CyclinD1 pathway in pancreatic cancer cells. (A) Colony-forming assay to examine the effects of knocking down YTHDF2 on the growth of SW1990 and BxPC3 cells. *** $P < 0.001$. (B) SW1990 and BxPC3 cells were transfected with sh-EGFP or sh-YTHDF2#1/ sh-YTHDF2#2 plasmid and the number of viable cells at the indicated time points was evaluated using the Cell Count Kit-8. The proliferation of cells was suppressed by YTHDF2 depletion. ** $P < 0.01$. (C) Immunoblotting of Akt, p-Akt, GSK3 β , p- GSK3 β , CyclinD1 in SW1990 and BxPC3 cells treated with sh-YTHDF2#1 or sh-EGFP. β -Tubulin was used as a loading control. (D, E) YTHDF2 knockdown in SW1990 and BxPC3 increased the fraction of cells in G1/G0-phase with a corresponding decrease in S-phase as compared to the control cells. Data are expressed as mean \pm SD. The results are representative of three independent experiments. Data are expressed as mean \pm SD. The results are representative of three independent experiments.

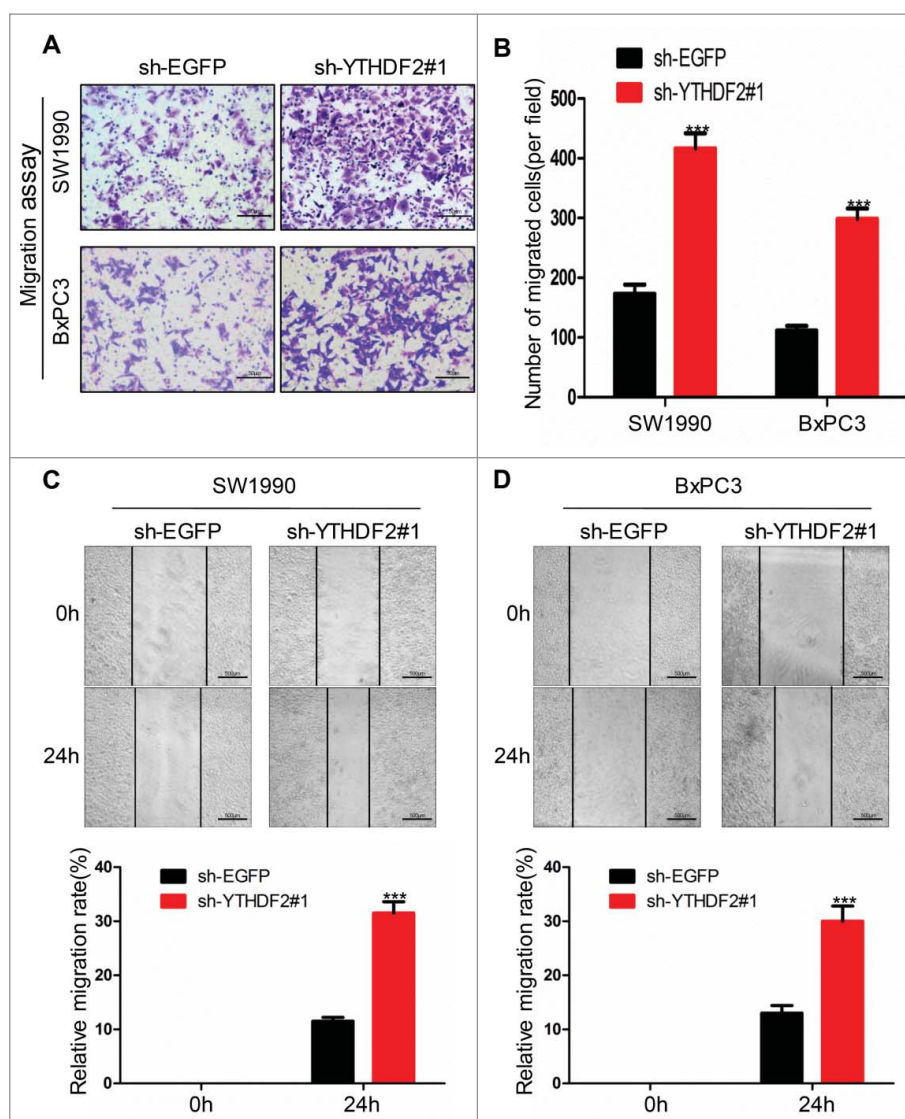


Figure 4. YTHDF2 knockdown promotes the migration ability of pancreatic cancer cells. (A) The ability of migration was examined using transwell assay in SW1990 and BxPC3 cells transfected with sh-YTHDF2#1 or sh-EGFP plasmids. Representative images of migrated cells were shown. Magnification, $\times 20$; bars, $50 \mu\text{m}$. (B) The graph indicated the average number of migrated cells per field. $***P < 0.001$. (C, D) A scrape wound was created in confluent cultures of SW1990 and BxPC3 cells with stable expression of either sh-YTHDF2#1 or sh-EGFP, the distance of cell migration was recorded and the relative migration rate was calculated. $***P < 0.001$. Data are expressed as mean \pm SD. The results are representative of three independent experiments.

YAP, p-YAP (Fig. 6C). To confirm that YTHDF2 knockdown promotes EMT via YAP in pancreatic cancer cells, we transfected stable cell lines-SW1990 and BxPC3 cells with sh-EGFP or sh-YAP. Our results revealed that YAP knockdown reversed the change mediated by YTHDF2 knockdown (Fig. 6D). All these findings indicate that YTHDF2 knockdown induces EMT probably via up-regulation of total YAP in pancreatic cancer cells.

YTHDF2 is up-regulated in other cancers

To confirm the clinical relevance of YTHDF2 expression in other cancers, we analyzed the mRNA levels of YTHDF2 from oncomine (www.oncomine.org). We found significant elevation of YTHDF2 expression levels in tumor tissues compared to non-tumor tissues (gastric mucosa $n = 31$; gastric intestinal type adenocarcinoma $n = 26$; $P < 0.001$, Fig. 7A), (brain non-tumor tissue $n = 10$; brain glioblastoma $n = 542$; $P < 0.001$,

Fig. 7B), (lung tissue $n = 58$; lung adenocarcinoma $n = 58$; $P < 0.001$, Fig. 7C), (liver non-tumor tissue $n = 220$; hepatocellular carcinoma $n = 225$; $P < 0.001$, Fig. 7D). All these data indicate that YTHDF2 mRNA expression is significantly up-regulated in other cancers.

Discussion

In this study, our findings suggest the dual function of YTHDF2 in pancreatic tumor progression, one for promotion and the other for suppression. We for the first time find that YTHDF2 orchestrates proliferation and epithelial-mesenchymal transition dichotomy in pancreatic cancer cells. Importantly, we confirm that YTHDF2 is up-regulated in human pancreatic cancer at both mRNA and protein levels, and acts as an independent impact factor for patient's poor stage. All these findings suggest that YTHDF2 may be a candidate for diagnosis and prognosis of pancreatic cancer.

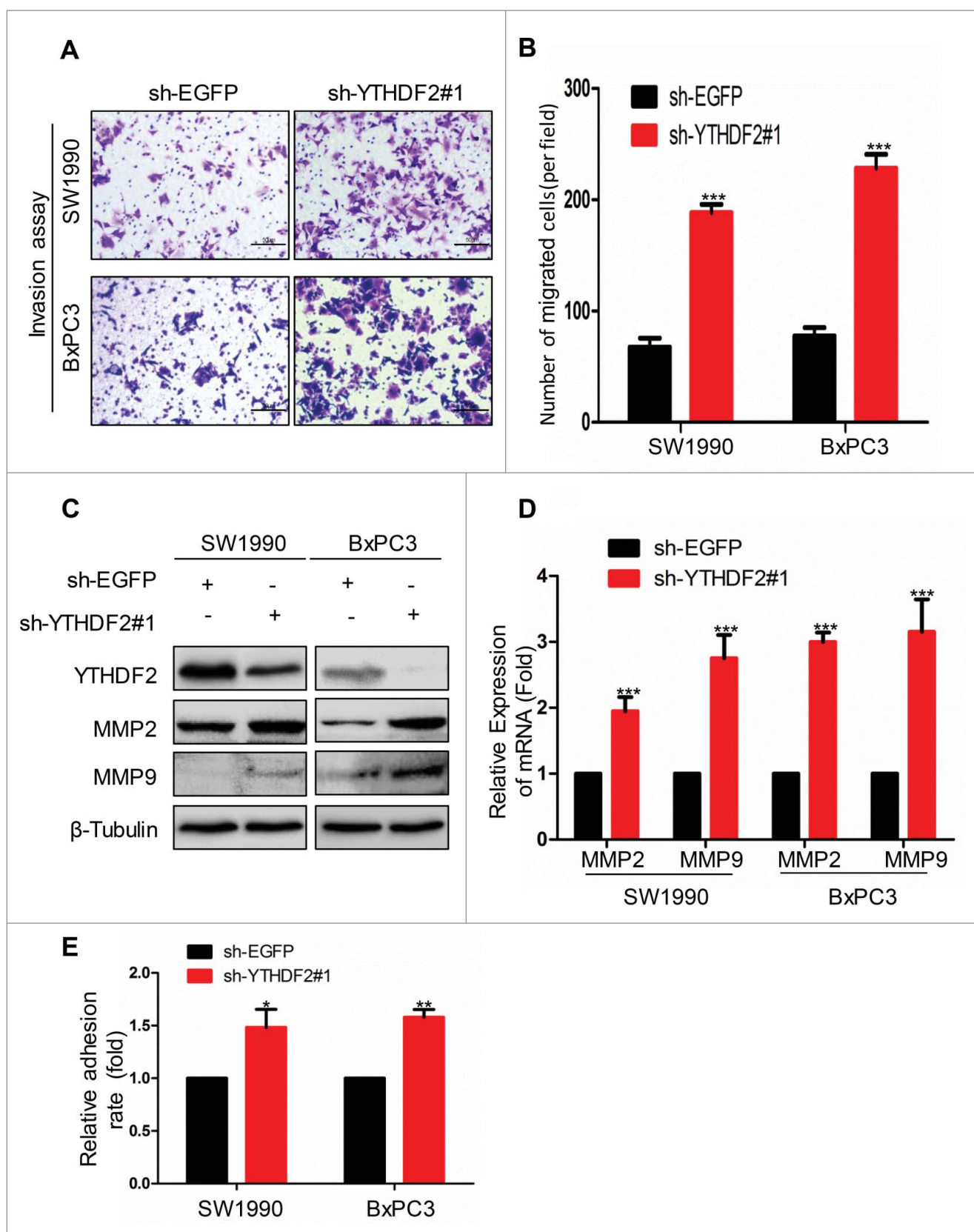


Figure 5. YTHDF2 knockdown promotes the invasion and adhesion ability in pancreatic cancer cells. (A) The invasion ability was examined using BD Matrigel invasion assay in SW1990 and BxPC3 cells transfected with sh-EGFP or sh-YTHDF2#1 plasmids. Magnification, $\times 20$; bars, $50 \mu\text{m}$. (B) Invasive cells were counted and analyzed. $***P < 0.001$. (C, D) MMP2 and MMP9 were identified using western blotting and real-time PCR in above cells. $***P < 0.001$. (E) The ability of adhesion was examined using cell adhesion assay in SW1990 and BxPC3 cells transfected with sh-YTHDF2#1 or sh-EGFP plasmids. β -Tubulin was used as a loading control. Data are expressed as mean \pm SD. The results are representative of three independent experiments.

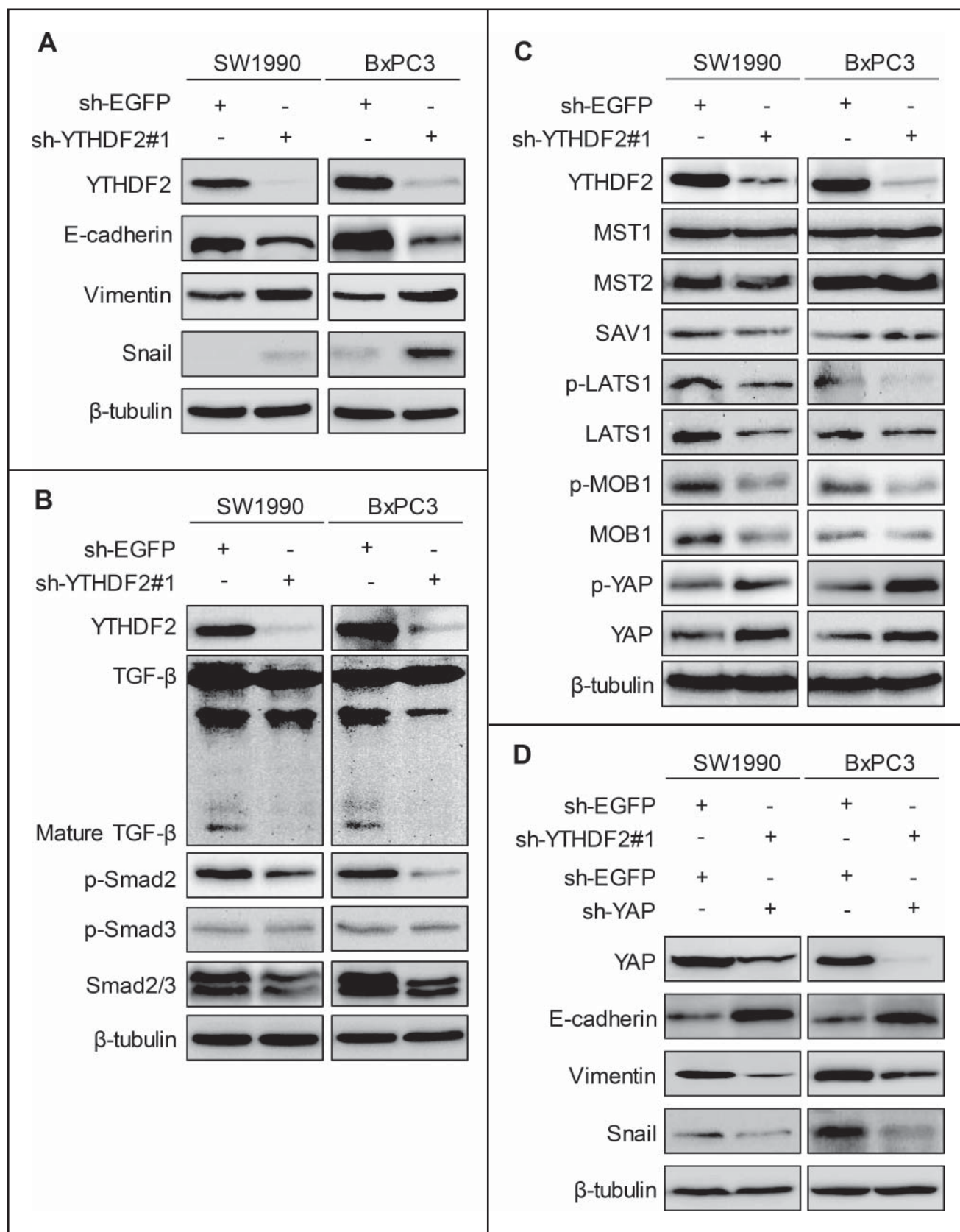


Figure 6. YTHDF2 knockdown promotes EMT through up-regulating of the total YAP expression. (A) Knockdown of YTHDF2 in SW1990 and BxPC3 cells induced EMT, as detected by increases in Vimentin, Snail and a decrease in E-cadherin. (B) Knockdown of YTHDF2 down-regulated the mature TGF- β , Smad2/3, p-Smad2. (C) Knockdown of YTHDF2 down-regulated the LATS1, p-LATS1, MOB1, p-MOB1 and up-regulated the YAP, p-YAP. (D) Knockdown of YAP in stable cell lines-SW1990 and BxPC3 cells up-regulated the E-cadherin and down-regulated the YAP, Vimentin and Snail. β -Tubulin was used as a loading control. Data are expressed as mean \pm SD. The results are representative of three independent experiments.

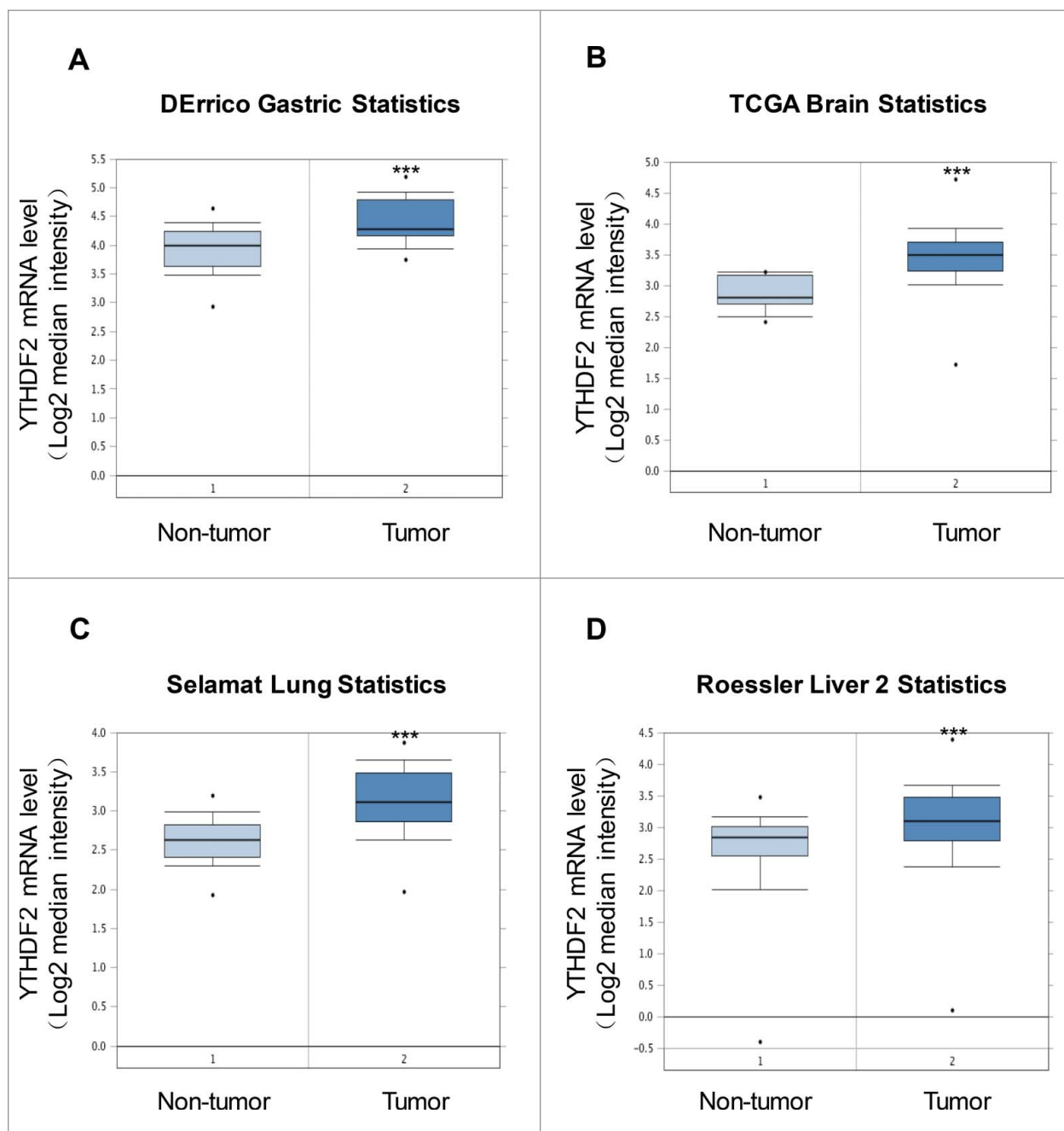


Figure 7. YTHDF2 is up-regulated in other cancers. (A) Analysis of YTHDF2 mRNA levels in 57 samples of gastric intestinal type adenocarcinoma and non-tumor tissues. N = 31 for non-tumor group, and N = 26 for tumor group. $***P < 0.001$. (B) Analysis of YTHDF2 mRNA levels in 552 samples of brain glioblastoma and non-tumor tissues. N = 10 for non-tumor group, and N = 542 for tumor group. $***P < 0.001$. (C) Analysis of YTHDF2mRNA levels in 116 samples of lung adenocarcinoma and non-tumor tissues. N = 58 for non-tumor group, and N = 58 for tumor group. $***P < 0.001$. (D) Analysis of YTHDF2 mRNA levels in 445 samples of hepatocellular carcinoma and non-tumor tissues. N = 220 for non-tumor group, and N = 225 for tumor group. $***P < 0.001$.

Uncontrolled proliferation and abnormal cell migration are two of the main characteristics of tumor growth.^{16,17} Cells respond to gene alterations by either proliferating or migrating, but not both at the same time, a phenomenon termed migration-proliferation dichotomy.¹⁸ This dichotomy has been reported that Girdin has dual function: it enhances the migration but suppresses the proliferation of cancer cells.^{18,19} Similar to our observations, depletion of Dlg5 in prostate and pancreatic cancer cells resulted in an attenuation of cell proliferation in addition to enhanced cell migration.²⁰ In this study, we at the first time report that YTHDF2 promotes the ability of proliferation and suppresses the abilities of migration and invasion

in pancreatic cancer. The dual roles of YTHDF2 provide an appropriate example in support of the theory of migration-proliferation dichotomy. The underlying mechanism of this phenomenon has remained several kinds of views. One argument is that the reciprocal and coordinated suppression/activation of transcription factors underlies the dichotomy between proliferation and invasion.²¹ Another argument is that the exhaustion of diffusion-driven oxygen environment of tumor cells can then result in the emergence of highly motile tumor cells.²² The researchers have made some attempts to apply the type of genes for the treatment of cancer. Inhibition of G6PD decreases cell proliferation but increases migration. G6PD knockdown in a

highly proliferative but noninvasive glioblastoma cell line resulted in prolonged survival of mice with intracerebral xenografts.²³ The specific treatment, according to the tumor behavior characteristics may become the new strategy for cancer treatment for “go or grow” status.

Pancreatic carcinoma is one of the most malignant tumor diseases.²⁴ It is believed that the high invasiveness of pancreatic cancer cells plays a critical role in the disastrous prognoses associated with this disease.^{25,26} EMT is a pivotal biological process in cancer progression that enables the initial tumor cells to obtain invasive and metastatic properties.²⁷ E-cadherin, an important glycoprotein of the classical cadherin members, regulates cell adhesion in normal adult epithelial cells. Loss of E-cadherin expression is considered to promote tumor invasion and metastasis, which can function as a marker of EMT.²⁸ However, Vimentin, a component of intermediate filaments, functions as a positive regulatory marker of EMT by up-regulating several EMT-related genes.²⁹ In our research, YTHDF2 was shown to inhibit the EMT phenotype of pancreatic cancer cells. We believe that this finding indicates that YTHDF2 is a key regulator of EMT and restrains the ability of migration and invasion in tumor cells. Additionally, abundant researches have shown that TGF- β can induce EMT.¹³ Therefore, we examine the key protein of the TGF- β /Smad signaling pathway, and found that YTHDF2 knockdown suppresses TGF- β /Smad signaling in pancreatic cancer cells. The YTHDF2 knockdown-induced expression of mesenchymal makers is independent of canonical TGF- β /Smad signaling. It has been proved that YAP overexpression resulted in the decrease expression of epithelial markers and increase of mesenchymal markers, whereas silencing YAP reversed them.³⁰ In this study, we found that YAP was inversely associated with YTHDF2 in pancreatic cancer cells. These findings indicate that YTHDF2 inhibits EMT in pancreatic cancer cells probably through YAP suppression. It has been reported that the phosphorylation of LATS1 is enhanced by the presence of MOB1. Activated LATS1 then phosphorylates and inactivates the downstream transcriptional co-activator YAP in mammals.³¹ Therefore, we speculate that YTHDF2 might contribute to activate the upstream molecules of YAP. Previous studies have shown that there are two m⁶A sites in YAP with one site in CDS and the other site in exon.³² Thus, it is reasonable to suppose that YTHDF2 might directly bind to YAP mRNA to decrease the stability of mRNA. However, the direct link between YTHDF2 and YAP in pancreatic cancer cells remains to be clarified.

In summary, our study provides proof that YTHDF2 orchestrates proliferation and epithelial-mesenchymal transition dichotomy in pancreatic cancer cells. YTHDF2 has the potential value to be developed as a new target for pancreatic cancer prevention and therapy.

Materials and methods

Cells and cell culture

Pancreatic cancer cell lines SW1990, PaTu8988 and BxPC3 were purchased from the Type Culture Collection of the Chinese Academy of Sciences, Shanghai, China. Meanwhile, the human embryonic kidney cell line (293T) was acquired from

the American Type Culture Collection. All cell lines were cultured in DMEM (Hyclone, China) supplemented with 10% fetal bovine serum (Gibco, USA), 100mg/L penicillin at 37°C in a humidified incubator with 5% CO₂ supply.

Western blotting

The cultured cells were rinsed with cold PBS before treated with 1 × SDS loading buffer at 100°C for 10 min. Then the mixture was centrifuged at 12000 r/min for 5 min. About 10 μ l of protein was loaded each lane, and separated by 10% SDS-PAGE and then transferred to the PVDF membrane. The membrane was blocked by 5% non-fat milk powder for 1 h at room temperature and then incubated with primary antibodies at 4°C overnight. The membranes were washed with TBS-T buffer (10 mMTris-HCl, pH 7.4, 150 mMNaCl, 0.05% Tween 20) for 15 min and incubated with HRP-labeled secondary antibodies. The antibodies were rabbit anti-YTHDF2 (Proteintech, 24744-1-AP), mouse anti- β -Tubulin (Cell Signaling, CAT 6181), rabbit anti-E-Cadherin (Cell Signaling, CAT 3195), rabbit anti-Vimentin (Cell Signaling, CAT 5741), rabbit anti-Snail (Cell Signaling, CAT 3879), rabbit anti-TGF- β (Cell Signaling, CAT 3711), rabbit anti-Smad2/3 (Cell Signaling, CAT 8685), rabbit anti-p-Smad2 (Cell Signaling, CAT 3108), rabbit anti-p-Smad3 (Cell Signaling, CAT 9520), rabbit anti-MMP2 (ImmunoWay, CAT YT2798), rabbit anti-MMP9 (ImmunoWay, CAT YT1892), rabbit anti-MST1 (Cell Signaling, CAT 3682), rabbit anti-MST2 (Cell Signaling, CAT 3952), rabbit anti-SAV1 (Cell Signaling, CAT 13301), rabbit anti-p-MOB1 (Cell Signaling, CAT 8699), rabbit anti-MOB1 (Cell Signaling, CAT 13730), rabbit anti-p-LATS1 (Cell Signaling, CAT 8654), rabbit anti-LATS1 (Cell Signaling, CAT 3477), rabbit anti-p-YAP (Cell Signaling, CAT 13619), rabbit anti-YAP (Cell Signaling, CAT 8418), rabbit anti-Akt (Cell Signaling, CAT 4691), rabbit anti-p-Akt (Cell Signaling, CAT 4060), rabbit anti-GSK3 β (Cell Signaling, CAT 12456), rabbit anti-p-GSK3 β (Cell Signaling, CAT 5558), rabbit anti-CyclinD1 (Cell Signaling, CAT 2978), mouse anti-PKA (Santa Cruz Biotechnology, SC-271125), rabbit anti-p-PKA (Bioss Biotechnology, BS4345), mouse anti-ILK (Santa Cruz Biotechnology, SC-20019).

Real-time PCR

We extracted total RNA using RNAiso Plus (Takara). Reverse transcription was performed using RevertAid First Strand cDNA Synthesis Kit (Thermo) according to the manufacturer's specification. Real-time PCR was performed in triplicate in 20 μ l reactions with iQ SYBR[®] Premix Ex Taq[™] Perfect Real Time (Bio-Rad Laboratories, Inc.), 50 ng first strand cDNA and 0.2 μ g each primer. The primer pair used for the amplification of the human YTHDF2 gene was as follows: forward primer, 5'-TAGCCAACTGCGACACATTC-3', and reverse primer, 5'-CACGACCTTGACGTTCCCTTT-3'. MMP2 primer: Forward, 5'-CACAGGAGGAGAAGGCTGTG-3' and reverse, 5'-GAGCTTGGGAAAGCCAGGAT-3'; MMP9 primer: Forward, 5'-TTCAGGGAGACGCCCATTTTC-3' and reverse, 5'-TG TAGAGTCTCTCGCTGGGG-3'; and GAPDH primer: Forward, 5'-GGTGAAGGTCGGTGTGAACG-3' and reverse, 5'-CTCGCTCCTGGAAGATGGTG-3'. Samples were cycled once

at 95°C for 2 min, then subjected to 35 cycles of 95°C, 56°C and 72°C for 30 sec each. The relative fold change in RNA expression was calculated using the $2^{-\Delta\Delta Ct}$ method with GAPDH as an endogenous control.

Plasmid construction

The entire YTHDF2 sequence was amplified with RT-PCR using primers YTHDF2-all-F: 5'-GAGGCGATCGCATGTCCG CCAGCAGCCTCTT-3', and YTHDF2-all-R: 5'-GCGACGC

GTTTTCCACGACCTTGACGTTCTT-3', and then inserted into the AsiSI and MluI site of the pCMV6-Entry plasmid (Origene) and ligated into the vector. The YTHDF2 and EGFP shRNA oligos (YTHDF2-shRNA#1-F 5'-CCGGGCTAC TCTGAGGACGATATTCCTCGAG

GAATATCGTCTCAGAGTAGCTTTTTG-3', YTHDF2-shRNA#1-R 5'-AATTCAAAAA

GCTACTCTGAGGACGATATTCCTCGAGGAATATCGT CCTCAGAGTAGC-3', YTHDF2-shRNA#2-F 5'-CCGGCGGT CCATTAATAACTATAACCTCGAGGTTATAGTTA

TTAATGGACCGTTTTG-3', YTHDF2-shRNA#2-R 5'-AATTCAAAAAACGGTCCATTA

TAACTATAACCTCGAGGTTATAGTTATTAATGGACC G-3', YAP-shRNA-F5'-CCGGCC

CAGTTAAATGTTACCAATCTCGAGATTGGTGAACA TTAACTGGGTTTTG-3', YAP-shRNA-R 5'-AATTCAAAA AACCCAGTTAAATGTTACCAATCTCGAG ATGGTG

AACATTTAACTGGG-3', EGFP-shRNA-F 5'-CCGGTACA ACAGCCACAACGTCTATCT

CGAGATAGACGTTGTGGCTGTTGTATTTTTG-3', EGF P-shRNA-R 5'-AATTCAAAAA

TACAACAGCCACAACGTCTATCTCGAGATAGACGTT GTGGCTGTTGTA-3') were firstly annealed into double strands and then cloned into pLKO.1-puro (Sigma).

Transfection

Cells were transfected with plasmid DNA or shRNA using lipofectamineTM2000 Reagent (Invitrogen) following the manufacturer's protocol.

Generation of stable cell lines

To produce cells that constitutively expressed small hairpin RNA or short hairpin RNA (shRNA). The packaging plasmid psPA × 2 and the envelope plasmid pMD2.G were purchased from Sigma (MO, USA). PLKO.1-sh-YTHDF2 vector was co-transfected with psPA × 2 and pMD2.G into HEK293T cells using Lipofectamine 2000 (Invitrogen). Viruses were harvested 48 h and 72 h after transfection and viral titers were determined. Cells were infected with 1×10^6 recombinant lentivirus transduction units in the presence of 8mg/mL polybrene (Sigma, MO, USA). Puromycin ($1 \mu\text{g} / \text{mL}$) was added to cells until the cells in blank group died off. The survival cells were stable infected cells.

Cell Counting Kit-8 assay

The measurement of viable cell mass was performed with Cell Counting Kit-8 (Promega) according to manufacturer's

instructions. Briefly, 1000 cells/well were seeded in a 96-well plate and grew in an incubator (5% CO₂, 37°C). 10 μl CCK-8 was added to each well respectively in the first six days, and cells were incubated at 37°C for 2 h and the absorbance was finally determined at 490 nm.

Colony-forming assay

Stable cell lines-SW1990 and BxPC3 cells were harvested, resuspended in medium and were transferred to the six well plate (500, 1000, 2000 cells per well) for 10–14 days until large colonies were visible. Colonies were fixed in 4% paraformaldehyde for 30 min and then stained with 0.05% crystal violet for 30min, and the number of colonies was counted or photomicrographs were taken under phase-contrast microscope.

Wound Healing assay

Cells have grown to confluence in complete cell culture medium. At time 0h, a scrape wound was created across the diameter with a 10- μl pipette tip followed by extensive washes with medium to remove dead and floating cells. The distance was recorded at 0 and 24 h. Images were captured using an inverted microscope equipped with a digital camera.

Migration assay and invasion assay

For assessing cell migration, 5×10^5 cells in serum free media were seeded into the transwell inserts (Corning) containing 8- μm permeable pores and were allowed to migrate toward 10% FBS-containing medium. 36~48 h later, the migrated cells on the bottom of the insert were fixed with 4% paraformaldehyde solution followed by crystal violet (1%) staining. Pictures were taken after washing the inserts three times with PBS. Five independent fields were counted for each transwell and the average numbers of cells/field were represented in the graphs. For assessing cell invasion, 5×10^5 cells in serum-free medium were seeded in the transwell inserts which had already been covered with a layer of BD Matrigel Basement Membrane. The cells were later processed similar to that of cell migration assay. Finally, invaded cells were counted and the relative number was calculated.

Cell adhesion assay

Briefly, 96 well plates were coated with a layer of BD Matrigel using the manufacture's procedure. 4×10^4 cells/well were seeded in a 96-well plate and grew in an incubator. To allow the cells to attach, the plate was incubated at 37°C for 2 h. Non-adherent cells were removed by carefully aspirating the supernatant and rinsing with PBS. Complete growth media containing 10 μl CCK-8 was then introduced and incubated for 2 h (37°C) and the absorbance was finally determined at 490nm.

Cell cycle analysis

Transfected and treated cells were incubated 5 min at 37°C in lysis buffer with Hoechst (Chemometec). Thereafter, cells

received stabilizing buffer, before they were analyzed on a Nucleo Counter 3000 (Chemometec) for DNA quantitation in three independent experiments.

Retrospective analysis of YTHDF2 gene expression in human cancer

Correlations between pancreatic cancer pathologicT, stage and YTHDF2 gene expression were determined through analysis of GEO and TCGA databases, which are available through NCBI (<https://www.ncbi.nlm.nih.gov>) and UCSC (<https://genome-cancer.ucsc.edu>). YTHDF2 protein expression in pancreatic cancer tissues and normal tissues was determined from the human protein atlas (www.proteinatlas.org). YTHDF2 mRNA expression in gastric, brain, lung, liver cancer tissues and normal tissues were determined through analysis of DERICO, TCGA, Selamat and Roessler datasets respectively which are available through Oncomine (Compendia Biosciences, www.oncomine.org).

Statistical analysis

All grouped data is presented as mean \pm standard error. Differences between groups were assessed by ANOVA or Student's *t*-test using GraphPad Prism5 software. Differences with *P* values less than 0.05 were considered significant.

Conflict of interest

No potential conflict of interest was reported by the authors.

Acknowledgments

This study was supported by grants from the National Natural Science Foundation of China (81472333, 81372718, 81672402) and the Natural Science Foundation of Jiangsu Province (BK20131247).

References

- [1] Mazur PK, Herner A, Mello SS, Wirth M, Hausmann S, Sanchez-Rivera FJ, Lofgren SM, Kuschma T, Hahn SA, Vangala D, et al. Combined inhibition of BET family proteins and histone deacetylases as a potential epigenetics-based therapy for pancreatic ductal adenocarcinoma. *Nat Med*. 2015;21:1163-71. doi:10.1038/nm.3952. PMID:26390243
- [2] Roberts NJ, Norris AL, Petersen GM, Bondy ML, Brand R, Gallinger S, Kurtz RC, Olson SH, Rustgi AK, Schwartz AG, et al. Whole Genome Sequencing Defines the Genetic Heterogeneity of Familial Pancreatic Cancer. *Cancer Discov*. 2016;6:166-75. doi:10.1158/2159-8290.CD-15-0402. PMID:26658419
- [3] Schlomann U, Koller G, Conrad C, Ferdous T, Golfi P, Garcia AM, Höfling S, Parsons M, Costa P, Soper R, et al. ADAM8 as a drug target in pancreatic cancer. *Nat Commun*. 2015;6:6175. doi:10.1038/ncomms7175. PMID:25629724
- [4] Mayers JR, Wu C, Clish CB, Kraft P, Torrence ME, Fiske BP, Yuan C, Bao Y, Townsend MK, Tworoger SS, et al. Elevation of circulating branched-chain amino acids is an early event in human pancreatic adenocarcinoma development. *Nat Med*. 2014;20:1193-8. doi:10.1038/nm.3686. PMID:25261994
- [5] Wang X, Lu Z, Gomez A, Hon GC, Yue Y, Han D, Fu Y, Parisien M, Dai Q, Jia G, et al. N6-methyladenosine-dependent regulation of messenger RNA stability. *Nature*. 2014;505:117-20. doi:10.1038/nature12730. PMID:24284625
- [6] Maity A, Das B. N6-methyladenosine modification in mRNA: machinery, function and implications for health and diseases. *FEBS J*. 2016;283:1607-30. doi:10.1111/febs.13614. PMID:26645578
- [7] Zhu T, Roundtree IA, Wang P, Wang X, Wang L, Sun C, Tian Y, Li J, He C, Xu Y. Crystal structure of the YTH domain of YTHDF2 reveals mechanism for recognition of N6-methyladenosine. *Cell Res*. 2014;24:1493-6. doi:10.1038/cr.2014.152. PMID:25412661
- [8] Li F, Zhao D, Wu J, Shi Y. Structure of the YTH domain of human YTHDF2 in complex with an m(6)A mononucleotide reveals an aromatic cage for m(6)A recognition. *Cell Res*. 2014;24:1490-2. doi:10.1038/cr.2014.153. PMID:25412658
- [9] Zhang Z, Theler D, Kaminska KH, Hiller M, de la Grange P, Pudimat R, Rafalska I, Heinrich B, Bujnicki JM, Allain FH, et al. The YTH domain is a novel RNA binding domain. *J Biol Chem*. 2010;285:14701-10. doi:10.1074/jbc.M110.104711. PMID:20167602
- [10] Niu Y, Zhao X, Wu YS, Li MM, Wang XJ, Yang YG. N6-methyladenosine (m6A) in RNA: an old modification with a novel epigenetic function. *Genomics Proteomics Bioinformatics*. 2013;11:8-17. doi:10.1016/j.gpb.2012.12.002
- [11] Medina M, Wandosell F. Deconstructing GSK-3: The Fine Regulation of Its Activity. *Int J Alzheimers Dis*. 2011;2011:479249. PMID:21629747
- [12] Parvani JG, Gujrati MD, Mack MA, Schiemann WP, Lu ZR. Silencing beta3 Integrin by Targeted ECO/siRNA Nanoparticles Inhibits EMT and Metastasis of Triple-Negative Breast Cancer. *Cancer Res*. 2015;75:2316-25. doi:10.1158/0008-5472.CAN-14-3485. PMID:25858145
- [13] David CJ, Huang YH, Chen M, Su J, Zou Y, Bardeesy N, Iacobuzio-Donahue CA, Massagué J. TGF-beta Tumor Suppression through a Lethal EMT. *Cell*. 2016;164:1015-30. doi:10.1016/j.cell.2016.01.009. PMID:26898331
- [14] Jiang Y, Woosley AN, Sivalingam N, Natarajan S, Howe PH. Cathepsin-B-mediated cleavage of Disabled-2 regulates TGF-beta-induced autophagy. *Nat Cell Biol*. 2016;18:851-63. doi:10.1038/ncb3388. PMID:27398911
- [15] Shao DD, Xue W, Krall EB, Bhutkar A, Piccioni F, Wang X, Schinzel AC, Sood S, Rosenbluh J, Kim JW, et al. KRAS and YAP1 converge to regulate EMT and tumor survival. *Cell*. 2014;158:171-84. doi:10.1016/j.cell.2014.06.004. PMID:24954536
- [16] O'Leary B, Finn RS, Turner NC. Treating cancer with selective CDK4/6 inhibitors. *Nat Rev Clin Oncol*. 2016;13:417-30. doi:10.1038/nrclinonc.2016.26. PMID:27030077
- [17] Harney AS, Arwert EN, Entenberg D, Wang Y, Guo P, Qian BZ, Oktay MH, Pollard JW, Jones JG, Condeelis JS. Real-Time Imaging Reveals Local, Transient Vascular Permeability, and Tumor Cell Intravasation Stimulated by TIE2hi Macrophage-Derived VEGFA. *Cancer Discov*. 2015;5:932-43. doi:10.1158/2159-8290.CD-15-0012. PMID:26269515
- [18] Ghosh P, Beas AO, Bornheimer SJ, Garcia-Marcos M, Forry EP, Johansson C, et al. A G i-GIV Molecular Complex Binds Epidermal Growth Factor Receptor and Determines Whether Cells Migrate or Proliferate. *Molecular Biology of the Cell*. 2010;21:2338-54. doi:10.1091/mbc.E10-01-0028. PMID:20462955
- [19] Lopez-Sanchez I, Garcia-Marcos M, Mittal Y, Aznar N, Farquhar MG, Ghosh P. Protein kinase C-theta (PKCtheta) phosphorylates and inhibits the guanine exchange factor, GIV/Girdin. *Proceedings of the National Academy of Sciences of the United States of America*. 2013;110:5510-5. doi:10.1073/pnas.1303392110. PMID:23509302
- [20] Tomiyama L, Sezaki T, Matsuo M, Ueda K, Kioka N. Loss of Dlg5 expression promotes the migration and invasion of prostate cancer cells via Girdin phosphorylation. *Oncogene*. 2014;34:1141-9. doi:10.1038/onc.2014.31. PMID:24662825
- [21] Hjelmeland AB, Dhruv HD, McDonough Winslow WS, Armstrong B, Tuncali S, Eschbacher J, et al. Reciprocal Activation of Transcription Factors Underlies the Dichotomy between Proliferation and Invasion of Glioma Cells. *PLoS ONE*. 2013;8:e72134. doi:10.1371/journal.pone.0072134. PMID:23967279
- [22] Tan X, Wang S, Yang B, Zhu L, Yin B, Chao T, Zhao J, Yuan J, Qiang B, Peng X. The CREB-miR-9 negative feedback microcircuitry coordi-

- nates the migration and proliferation of glioma cells. *PLoS One*. 2012;7:e49570. doi:10.1371/journal.pone.0049570. PMID:23185366
- [23] Kathagen-Buhmann A, Schulte A, Weller J, Holz M, Herold-Mende C, Glass R, Lamszus K. Glycolysis and the pentose phosphate pathway are differentially associated with the dichotomous regulation of glioblastoma cell migration versus proliferation. *Neuro-Oncology*. 2016;18:1219-29. doi:10.1093/neuonc/now024. PMID:26917237
- [24] Razidlo GL, Magnine C, Sletten AC, Hurley RM, Almada LL, Fernandez-Zapico ME, Ji B, McNiven MA. Targeting Pancreatic Cancer Metastasis by Inhibition of Vav1, a Driver of Tumor Cell Invasion. *Cancer Res*. 2015;75:2907-15. doi:10.1158/0008-5472.CAN-14-3103. PMID:25977335
- [25] von Karstedt S, Conti A, Nobis M, Montinaro A, Hartwig T, Lemke J, Legler K, Annenwarter F, Campbell AD, Taraborrelli L, et al. Cancer cell-autonomous TRAIL-R signaling promotes KRAS-driven cancer progression, invasion, and metastasis. *Cancer cell*. 2015;27:561-73. doi:10.1016/j.ccell.2015.02.014. PMID:25843002
- [26] Chronopoulos A, Robinson B, Sarper M, Cortes E, Auernheimer V, Lachowski D, Attwood S, Garcia R, Ghassemi S, Fabry B, et al. ATRA mechanically reprograms pancreatic stellate cells to suppress matrix remodelling and inhibit cancer cell invasion. *Nat Commun*. 2016;7:12630. doi:10.1038/ncomms12630. PMID:27600527
- [27] Tang B, Qi G, Tang F, Yuan S, Wang Z, Liang X, Li B, Yu S, Liu J, Huang Q, et al. Aberrant JMJD3 expression upregulates Slug to promote migration, invasion and stem cell-like behaviors in hepatocellular carcinoma. *Cancer Res*. 2016;76:6520-32. doi:10.1158/0008-5472.CAN-15-3029.
- [28] Liu L, Zhu XD, Wang WQ, Shen Y, Qin Y, Ren ZG, Sun HC, Tang ZY. Activation of beta-catenin by hypoxia in hepatocellular carcinoma contributes to enhanced metastatic potential and poor prognosis. *Clinical cancer research: an official journal of the American Association for Cancer Research*. 2010;16:2740-50. doi:10.1158/1078-0432.CCR-09-2610. PMID:20460486
- [29] Chen SC, Kung ML, Hu TH, Chen HY, Wu JC, Kuo HM, Tsai HE, Lin YW, Wen ZH, Liu JK, et al. Hepatoma-derived growth factor regulates breast cancer cell invasion by modulating epithelial-mesenchymal transition. *J Pathol*. 2012;228:158-69. doi:10.1002/path.3988. PMID:22247069
- [30] Pei T, Li Y, Wang J, Wang H, Liang Y, Shi H, Sun B, Yin D, Sun J, Song R, et al. YAP is a critical oncogene in human cholangiocarcinoma. *Oncotarget*. 2015;6:17206-20. doi:10.18632/oncotarget.4043. PMID:26015398
- [31] Yu FX, Zhao B, Guan KL. Hippo Pathway in Organ Size Control, Tissue Homeostasis, and Cancer. *Cell*. 2015;163:811-28. doi:10.1016/j.cell.2015.10.044. PMID:26544935
- [32] Meyer KD, Saletore Y, Zumbo P, Elemento O, Mason CE, Jaffrey SR. Comprehensive analysis of mRNA methylation reveals enrichment in 3' UTRs and near stop codons. *Cell*. 2012;149:1635-46. doi:10.1016/j.cell.2012.05.003. PMID:22608085